

THE EVALUATION OF THE RESISTANCE AGAINST CRACK EXTENSION
BY INSTRUMENTED HIGH VELOCITY IMPACT ON 3-POINTS BEND (DROP
WEIGHT TEAR TEST LIKE) SPECIMENS IN PARTICULAR OF LINEPIPE
STEEL IN THE DUCTILE RANGE USING GASGUN FACILITIES

H.C. van Elst

Department of Strength of Structural Materials,
Metal Research Institute TNO, Apeldoorn, The Netherlands

ABSTRACT

Using as striker a cylindrical steel projectile (600 mm length, 40 mm diameter, 5,7 kg mass), ejected from a compressed airgun at velocities of 70 to 80 m/sec, drop weight tear test like linepipe steel specimens were impacted between minus 80 and plus 20 degrees centigrade. This provided kinetic energies sufficient to fracture specimens up to 35 mm thickness and 85 mm ligament in the ductile range at fracture velocities of ca. 150 m/sec, being representative for those occurring when unstable shear fractures propagate in gas pressurized pipelines under steady state conditions. A photocell device allowed to record the velocity of the projectile striker just before, during and after impact. With the aid of high speed photography the rotation and translation of the specimen in time could be observed, as well as the crack extension. This was facilitated by a square mesh, applied to the specimen surface by a photochemical method. The crack propagation could moreover be followed by a high frequency electrical resistance measurement over the notch mouth. Straingages on the rollers of the support mounted on a 1400 kg mass cast iron wheeled ingot, allowed to record the momentum transfer from the specimen to these. From the observed data, using momentum and energy balance considerations, the energy dissipation as a function of crack length can be calculated, duly taking into account translational, vibrational and rotational kinetic energy obtained by the specimen. A special determination of the energy dissipation due to the penetration of the projectile into the specimen by testing specimens with nearly through ligament finally allowed an estimate of the resistance against fracture propagation, to be understood as the required dissipated energy per unit crack area.

KEYWORDS

Ductile fracture; fracture resistance; fracture propagation; linepipe steel; gas-gun; high velocity impact; high speed photography; electronic instrumentation; energy and momentum balance; crack velocity measurement.

NOMENCLATURE

Symbol:	refers to:	Symbol:	refers to:
a	cracklength	r	rotation factor; $r(h-a)$ = distance of rotation centre from crack tip
m	mass	S_0	initial half span of specimen
v	projectile velocity	S_0	momentaneous apparent half span of impacted specimen obtained by imaginary movement of rollers opposite to impact direction, till contact of lost contact between specimen and roller is re-established
f	displacement of impact point of specimen	λ	slit width of reflective layer on projectile
x	displacement of centre of gravity of specimen in impact direction	b	specimen thickness
y	displacement of centre of gravity of specimen transversal to impact direction	ΔT	maximal permanent elongation transversal to totally developed crack
ϕ	angular displacement of specimen-half	\bar{Y}	effective yield stress ($= \frac{1}{2}(UTS + \text{yield strength})$)
I	moment of inertia	c	deformation
U	elastic potential energy		
W	dissipated energy		
R	fracture resistance (=dissipated energy pro unit crack area)		
p	momentum		
P	load exerted		
t	time		
h	specimen height		
q	initial distance between centres of gravity of specimenhalves		
w	angular velocity = $\dot{\phi}$		

index:	to symbol:	refers to:	index:	to symbol:	refers to:
1	m,v	projectile	10	v	initial value of V_1 (before impact)
2	m,x,y,I, ϕ ,W	specimen	21	y,I, ϕ	specimenhalf 1
3	m,p	supports	22	y,I, ϕ	specimenhalf 2
0	S,b	initial value	23	P	specimen on support
b	e	thickness			

N.B. Other used symbols (with their indices) are defined in text.

INTRODUCTION

It has been demonstrated that a gas pressurized pipeline can sustain unstable propagation of a ductile fracture in a steady state way over large distances. Cf. Maxey and colleagues (1972). For the assessment of the capacity of the linepipe steel to prevent - or at least arrest - such fractures the knowledge of its fracture propagation resistance, i.e. the energy dissipation pro unit crack area, appears essential for the relevant analyses as e.g. by Dick, Jamieson and Walker (1974), Van Elst (1974), Hahn and colleagues (1973), Poynton (1974), Poynton and Fearnough (1972). Deformation controlled tearing of current fracture mechanics specimens in a hydraulic way, allows to evaluate such a resistance at low shear fracture speeds (Cottrell, 1977; Van Elst, 1979; Priest and others, 1977, 1978). Using high deformation rates as in impact tests the fracture velocity can be increased to values representative for pipeline failure, i.e. 150-200 m/sec in the ductile range. From arrested shear fracture in drop weight tear test specimens the impression was gained that for the relevant specimen geometry a nearly constant ratio of 1.7-2.0 occurred between arrested cracklength and induced deflection. Thus preference was given to increase the kinetic energy of the striker to the required level for achieving specimen separation by increase of the striker velocity to ca. 70 m/sec, rather than by increase of its mass. This striker velocity, still

remaining below the Von Karman velocity indeed generated fracture velocities of the required order. Recent work by others (Junker and Vogt, 1978) however, appears to demonstrate that at lower deflection rates, but with an overshoot of kinetic energy by increase of the striker mass (up to 2000 kg) ductile fracture velocities of this order can be likewise generated. The low mass, high velocity striker can be realized with a projectile (600 mm length, 40 mm diameter, 5.7 kg mass) ejected by a gasgun at 70 to 80 m/sec velocity. The required design, instrumentation and processing of the data is elaborated in EXPERIMENTAL.

MATERIAL

Linepipe steel plates A and D of 16, B and C of 32 mm thickness resp., showing separations in Charpy V test results, were at disposal¹. Table 1 gives the chemical composition.

TABLE 1 Chemical analysis in % of linepipe steel A, B, C, D.

	C	S	Si	Mn	P	Cr	Ni	Mo	Cu
A	0.082	0.005	0.32	1.58	0.015	0.02	0.28	0.13	0.008
B	0.066	0.007	0.33	1.57	0.024	0.01	0.27	0.14	0.008
C	0.066	0.006	0.33	1.56	0.026	0.01	0.26	0.14	0.008
D	0.080	0.005	0.30	1.51	0.014	0.02	0.27	0.12	0.008

From each steel plate drop weight tear test like specimens were prepared with dimensions 500 mm x 100 mm x thickness; these were provided with a single edge notch of 15 mm (or longer) having a 3 mm jewellers saw cut and with 0.3 mm width. A (square mm) mesh was applied to the specimen surfaces in a photochemical way, facilitating to record the development of deformation during and after testing.

EXPERIMENTAL

Mechanical Aspects

Gasgun. The special designed gasgun has as barrel a 5 m long smooth steel tube with 40 mm innerdiameter, which can be connected to a pressure vessel (of 80 liters and 40 bar) by a sluice valve, also serving as projectileholder (Fig. 1a). The volume capacity of the pressure vessel being about 10x the volume capacity of the barrel implies a nearly constant pressure of the air driven projectile, during acceleration. As a consequence a comparatively low air pressure (40 bar) can be used to obtain impact energies sufficient to fracture 3-points bend specimen of linepipe steel up to thickness of 35 mm for 450 mm span width, 100 mm height and 15 mm (or larger) notch depth. If the projectile is in its holder the air supply is closed (Fig. 1b). The space behind the projectile is evacuated, causing the projectile to be inserted into its holder. Triggering occurs by rising the pressure in this space; this causes the projectile to leave its rest position, at the same time opening the connection to the compressed air supply, which results in its acceleration. The maximum kinetic energy that can be obtained will be restricted by the applied gas pressure and barrel dimensions (In crude approximation it will be of the order of gas pressure (40 bar) x barrellength (5m) x barrel cross section (12.56 mm²) i.e. 25 kJ). However, above a certain gaspressure the kinetic energy no longer increases. For the used projectile with 5.7 kg mass and its 80 m/sec attained velocity the kinetic energy reached by the projectile was ca. 18 kJ.

¹These were kindly set available by "Centro Sperimentale Metallurgico" Rome.

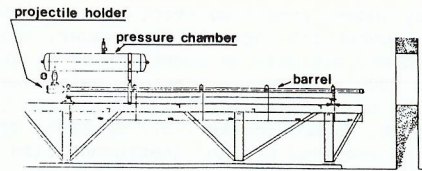


Fig. 1a. Gasgun for high velocity impact test

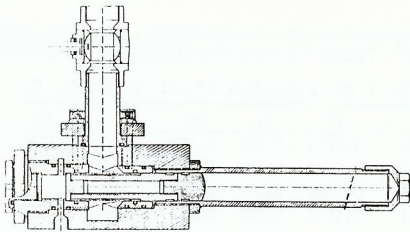


Fig. 1b. The projectile holder

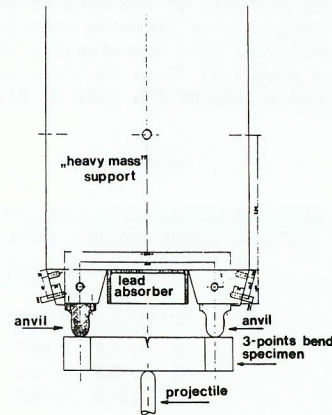


Fig. 1c. The supports and impact absorber

The support of the specimen. The supporting rollers of the 3-points bend specimen (450 mm span width, 100 mm height) are mounted on a 1400 kg mass especially cast iron buffer, which can roll on small wheels along rails in the impact direction (Fig. 1c). It is held in position by a spring; a shock absorber can exert forces on this buffer rapidly bringing down its possible movement. After fracture the projectile and both specimen parts are caught into a lead filled pan, reducing (specimen) damage. The support on the buffer is situated in a small concrete bunker of 2m x 2m x 2m, which can be completely closed only leaving entries for the projectile and the recording outputs.

Impact velocity aspects. For chosen dimensions and geometry of 3-points bend (e.g. drop weight tear test like) specimens a constant ratio between induced crack extension and enforced deflection will occur for a given ductility of the material, which can (slightly) depend on the displacement velocity. (Presumably this ratio is 0 for a rigid and ∞ for an ideal plastic specimen). As was already mentioned it appeared from arrested fractures in conventionally performed drop weight tear tests and from those provisionally performed with the gasgun, that for linepipe steel this ratio is between 1.7 and 2.0. This would imply that a deflection speed of ca. 70 m/sec would correspond to a crack velocity of ca. 140 m/sec, as could be verified (see below). The projectile caused a partial piercing of the specimen at impact, accompanied by excessive plastic deformation. It could be observed that this largely proceeds the initiation of the crack extension. The dissipated energy connected with this, unfavorably interfered with the aimed determination of the netto energy dissipation required for crack area realization, when the crack extends from the notch tip towards the opposite edge impacted by the striker. Also the ligament of interest available for crack extension decreases. With the aid of aluminium plates of 50 x 50 x 50 mm, sometimes copper or stainless steel plates, mounted in front of the specimen at the impact location and acting as a buffer, the energy dissipation of the specimen at impact can be reduced. This causes a more gradual acceleration of the specimen, yet achieving the high deflection rate as required. In this way a surpassing of the Von Karman velocity by the displacement which otherwise would have caused fracture transversal to the impact direction, can be overcome. However, fragmentation of such buffers and impact instability often

unfavorably interfered and their use remained scarce.

Instrumentation

Recording of the striker velocity. The path of the projectile was contactless recorded; two methods were used:

- a. A reflective layer slitted in strips of equal width was glued to the surface of the projectile. The light beam of an electronic optical scanner was focused on the position of these slits just before, during and (till shortly) after impact of the projectile. The recorded reflection time τ of a slit with width λ offers the velocity $v_1 = \lambda/\tau$ (and the deceleration of the projectile by differentiation in time).
- b. An array of $33 \times 3 = 99$ phototransistors with initial distance in impact direction of 1 mm is mounted below and near the projectile path just before the location of impact. These phototransistors are illuminated by a suitable adjusted light source above the projectile path. When the projectile passes along, it casts its shadow on these phototransistors. If the signal of an illuminated phototransistor corresponds to 1 and that of one in shadow to 0, the front and rear of the projectile position will correspond to a (0,1) or (1,0) situation of neighbouring phototransistors. The phototransistor pair below the projectile will have (0,0), before and after it (1,1) combination. Each pair of neighbouring phototransistors is monitored by an "exclusive or" circuit. This reads + at an unequal state of the neighbouring phototransistors, i.e. to a (0,1) or (1,0) combination of these and - in the alternative case. By making additional electronic distinction between the order of the unequal states, i.e. between (0,1) or (1,0) combinations of the phototransistor pairs by - or + respectively, moreover signals only referring to the rear position of the projectile were recorded (this was for obvious reasons preferred to reference to the front of the projectile). From all "exclusive or" circuits only one will be +, when the projectile passes, recording its rear position. This proceeded from 20 mm distance before impact onwards till total separation of fractured specimen parts. The description of the projectile path in time offers its velocity and deceleration in principle as well. The impact signal was recorded as time 0, using a breaking wire technique.

Recording of the crack extension. Both high speed electrical and photographic techniques were used.

- a. The recording of the crack extension by electrical means proceeded by coupling the notch opening to a (Hewlett-Packard 3310 B) function generator with a suitable transformer. This provided the matching impedance ($\approx 50 \Omega$) by increasing the load impedance ca. 400x. The primary of this transformer consists out of 20 turns around a ferrite core; the secondary is one turn around this, closed by the ligament via a printed (thus stiff) low impedance band conductor ca. 15 mm x 1.5 mm to the notch opening. By tuning to resonance, which occurred at 225 kHz (instead of the intended 1 MHz, due to the length of the required connecting cable, though this resonance frequency could have been easily increased if indicated), the Ohmic resistance of the secondary accounts for the impedance and this largely refers to the crack surface. For the skin effect will cause the current to flow near this surface and its enlargement at crack extension is readily detected. As the primary current amplitude will be a measure of the ohmic resistance in the secondary at resonance its measurement can proceed with a (Tektronix P 6042) current probe of which the output is demodulated and stored in a (Biomation model 805) transient recorder. From the obtained data it was concluded that the crack velocity was 100 m/sec, as could be verified by high speed photographic recordings.
- b. For the recording of the crack extension - and of the deflection, local deformations and rotation of specimen parts as well - by high speed photographic means a (Beckmann & Whitley Dynafax model 550) framing camera was applied in combination with a (Beckmann & Whitley model 358) electronic flash unit. This latter permits flash durations of 2.7; 5.4; 10.8 m sec with an output of 1.5×10^6 peak

beam candle power. The maximum framing speed is 35,000 f.p.s. with picture separations of 6 μsec and exposure times of 1.5 μsec; the total number of pictures is 48. The time link between the camera equipment and the electronic recordings was taken care off by signals from the camera, also indicating its framing speed by means of an electrical counter. The camera observations were made with a suitably mounted mirror under 45° with the impact direction.

The recording of the load. The load on the projectile can be found from its deceleration, i.e. by 2x differentiation of the path projectile recording in time. The load on the specimen supporting rollers was measured with straingages glued onto these.

THEORETICAL

For the specimen with mass m₂, impacted by a projectile with mass m₁ and velocity v₁₀, while supported by a heavy mass m₃, one will have as dissipated energy by the specimen:

$$W_2(a) = (\frac{1}{2}m_1v_{10}^2 - \frac{1}{2}m_1v_1^2)(1 - m_1/m_3) - \frac{1}{2}m_2\dot{x}_2^2(1 - m_2/m_3) + (m_1v_{10}v_1 + m_2v_{10}\dot{x}_2 + m_2v_1\dot{x}_2)m_1/m_3 - \frac{1}{2}(m_{21}\dot{y}_{21}^2 + m_{22}\dot{y}_{22}^2) - \frac{1}{2}(I_{21}\dot{\phi}_{21}^2 + I_{22}\dot{\phi}_{22}^2) - (U_1 + U_2 + U_3) = \frac{1}{2}m_1v_{10}^2 - \frac{1}{2}m_1v_1^2 - \{\frac{1}{2}m_2\dot{x}_2^2 + \frac{1}{2}(m_{21}\dot{y}_{21}^2 + m_{22}\dot{y}_{22}^2)\} - \frac{1}{2}(I_{21}\dot{\phi}_{21}^2 + I_{22}\dot{\phi}_{22}^2) \quad (1)$$

if terms with m₁/m₃ and also elastic energies are neglected.

- From the high speed photographic electronic recordings, it could be concluded:
- a. The projectile velocity rather abruptly drops after impact and then remains further constant. The apparent momentaneous transfer of kinetic energy from projectile to specimen, accounts for the energy dissipation by projectile penetration into the specimen, for generation of kinetic energy of the specimen viz. translational in x-direction, translational in both y-directions with algebraic angular momentum zero, for (here negligible) elastic potential energy and for the subsequent dissipation of energy (by conversion of the two latter "vibrational" energies as required by the crack extension. This crack extension starts before momentum transfer to the supports and clearly develops further during and after this.
 - b. The acceleration of the specimen caused by the impact of the projectile results in the former to move ahead of the latter with as a consequence the loss of contact of projectile and specimen.
 - c. The rotational momentums obtained by the impact of specimen and supports cause loss of contact between these too, as could be observed in the high speed photographic recordings. The translational displacement in x-direction subsequently causes again impact of specimen and supports; its corresponding momentum transfer was revealed by the load recordings with straingages glued to the rollers.

Substituting in (1):

$$\dot{x}_2 = (v_{10} - v_1)m_1/m_2 - p_3/m_2 \text{ with } p_3 = \int_{t_3}^t P_{23} dt'$$

(t₃ = time of impact between specimen and supports, when the projectile impact occurs at time 0; P₂₃ = load on supports by impact of specimen) one obtains:

$$W_2(a) = \frac{1}{2}m_1(v_{10}^2 - v_1^2) - \{m_1(v_{10} - v_1) - p_3\}^2/2m_2 - \frac{1}{2}I_2\dot{\phi}^2 - \frac{1}{2}(m_{21}\dot{y}_{21}^2 + m_{22}\dot{y}_{22}^2) \quad (2a)$$

$$= \frac{1}{2}m_1(v_{10}^2 - v_1^2) - \{m_1(v_{10} - v_1) - p_3\}^2/2m_2 - \frac{1}{2}I_2\dot{\phi}^2 - \frac{1}{2}m_2\zeta^2 \sin^2(\beta + \phi) \cdot \dot{\phi}^2 \quad (2b)$$

with B = B(h, g, a, r, \dot{a} , \dot{r} , $\dot{\phi}$); β = β(h, g, a, r, \dot{a} , \dot{r} , $\dot{\phi}$).

$$\dot{W}_2(a) = -I_2\dot{\phi}\ddot{\phi} - m_2BC\sin(\beta + \phi)\sin(\gamma + \dot{\phi}) \text{ with } C = C(h, q, a, r, \dot{a}, \dot{r}, \dot{\phi}, \ddot{a}, \ddot{r}, \ddot{\phi});$$

$$\gamma = \gamma(h, q, a, r, \dot{a}, \dot{r}, \dot{\phi}, \ddot{a}, \ddot{r}, \ddot{\phi}); \zeta, B, \beta, C \text{ and } \gamma \text{ are evaluated in APPENDIX .}$$

$$R(a, \dot{a}) = [-I_2\dot{\phi}\ddot{\phi} + \frac{1}{2}m_2BC(\cos(\beta + \gamma + \phi) - \cos(\beta - \gamma))] / b\dot{a}$$

If $\dot{\phi}, \ddot{a}, \ddot{r}, \ddot{\phi}$ can be neglected in a considered a-interval and ω = $\dot{\phi}$ (Cf. APPENDIX).

$$BC = [(\frac{1}{2}h - (1-r)(h-a))^2\omega^2 + \{-\frac{1}{2}q\omega + \dot{a}(1-r)\}^2]^{\frac{1}{2}} \cdot [(-\frac{1}{2}q\omega^2 + 2(1-r)\dot{a}\omega)^2 + \{\frac{1}{2}h - (1-r)(h-a)\}^2\omega^2]^{\frac{1}{2}}$$

In order to find the dissipated energy of interest, i.e. which is directly connected with crack extension (and possibly including that directly connected with crack initiation) one has still to subtract the dissipated energy caused by the penetration of the projectile into the specimen. By performance of experiments on specimens with only a rudimental ligament (of ca. 3 mm) one can find this latter energy from the loss of kinetic energy of the projectile and the acquired kinetic energy of the specimen (at φ = 0). This proves to be of the order of 4.5 kJ for the thicker specimens (corresponding with the observed hole of "40" mm diameter and 6 mm depth for an effective yield strength of ca. 600 MN/m² by plastic deformation). The reaction forces of the specimen halves on each other can only exist in y-direction, as these cannot change the momentum in x-direction for the relevant symmetrical case. For the specimen halves translating in opposite y-directions and rotating in opposite sense kinetic energies are generated as a consequence (the total algebraic momentum and total algebraic angular momentum remaining zero resp.). In absence of the supports, i.e. when impacting a freely suspended specimen, complete fracture was realized as well. From the high speed photographic recordings it proved in that case, that φ increases less in time, than when the supports can exert action, while φ decreased without supports. For the dissipated energy one will now have:

$$W_2(a) = \frac{1}{2}m_1(v_{10}^2 - v_1^2) - (v_{10} - v_1)^2 m_1^2 / 2m_2 - \frac{1}{2}I_2\dot{\phi}^2 - \frac{1}{2}m_2\zeta^2 \sin^2(\beta + \phi) \cdot \dot{\phi}^2 \quad (2c)$$

This evaluation bypasses occurring inaccuracies in p₃, while the terms with $\dot{\phi}^2$ are smaller in correspondence with the large x-translational kinetic energy of the specimen compared to experiments with supports. Presumably the error in φ causes the largest uncertainty in the W₂(a)-evaluation; in the latter equation this error is smaller in relative sense for the φ²-terms - and also for W₂(a).

RESULTS

Metallurgical characterization

Fracture appearances of not completely torn specimens, showing multiple arrest arrowheads due to separations, are shown in Fig. 2.

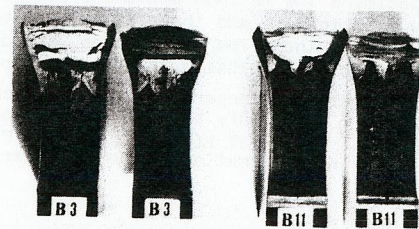


Fig. 2. Fracture appearance of not completely impact fractured specimens with thickness 30 mm tested at 20°C. Pronounced arrowheads in thickness halves at tip of arrested fracture revealed by heat staining and subsequently statically achieved complete separation.

By comparison of the fracture appearances of impact bend with slow quasi static bend tests the impression was gained that the increase of deformation rate enhanced the occurrence of separations; cf. Fig. 3a, 3b, 3c and 3d.

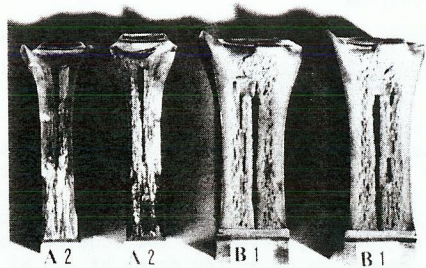


Fig. 3a. Dynamically tested specimens A₂ (16 mm), B₁ (30 mm); 20°C

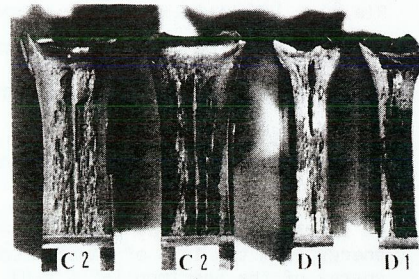


Fig. 3b. Dynamically tested specimens C₂ (30 mm), D₁ (16 mm); 20°C

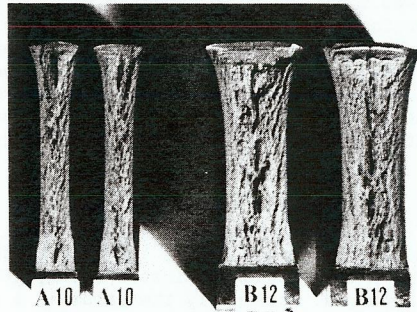


Fig. 3c. Statically torn specimens A₁₀ (16 mm), B₁₂ (30 mm); 20°C

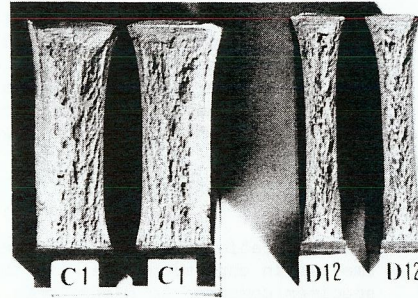


Fig. 3d. Statically torn specimens C₁ (30 mm), D₁₂ (16 mm); 20°C

Separation phenomena in linepipe steel are discussed by Engl and Fuchs (1978); this aspect is not further elaborated here.

Deformation measurements

For all tested specimens the maximum permanent elongation $\Delta\Gamma$ transversal to the crack, due to its plastic wake and the maximum reduction in thickness b/b_0 along the crackpath were determined. The elongations $2\Delta y_k$ of gage lengths $2y_{ok}$ transversal to the crack were plotted as a function of cracklength.

The $2\Delta y^* = \Delta\Gamma$ -values which no longer increased at increase of $2y_o^*$ were used for an R-estimate, taking $R = \frac{2}{3} \sqrt{3\Delta\Gamma}$; the maximum thickness reduction offered an R-estimate according to $R = \frac{2}{3} \sqrt{3Y} b(1-b/b_0)$. Cf. Van Elst (1979). Estimated R-values according to these deformation measurements are plotted as a function of temperature in Fig. 4.

Evaluations of dissipated energy and fracture resistance from balance considerations for energy and momentum using data obtained by high speed photographic and electronic recordings

Examples of relevant high speed photographic recordings are shown in Fig. 5, Fig. 6 and Fig. 7. Corresponding electronic recordings as shown in Fig. 8, reveal:

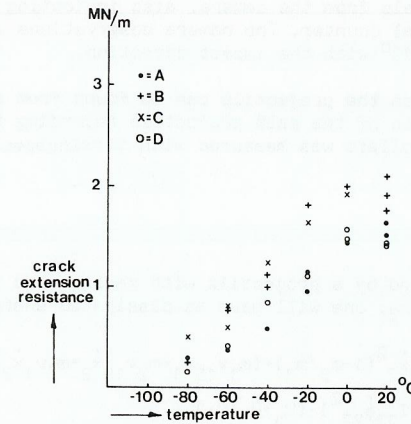


Fig. 4. R-estimate as a function of temperature from $\Delta\Gamma$ and b/b_0 measurements for 4 linepipe steels.

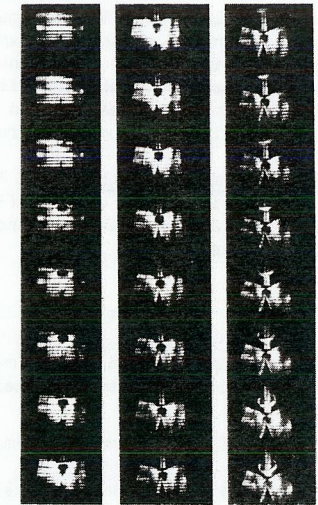


Fig. 5b. Selection of successive odd frames with 123,4 μ sec interval from a series of 48 high speed photographic recordings of gasgun high velocity impact bend tests; material B (30mm) at 20°C.



Fig. 6. Selection of successive odd frames from high speed photographic recordings of movement of specimen with initial nearly through ligament at gasgun high velocity impact bend test.



Fig. 7a. 48 successive frames by high speed photographic recording of movement of specimen without supports at gasgun high velocity impact bend test; material B (30mm) at 20°C; framing speed 66,5 μ sec/frame.

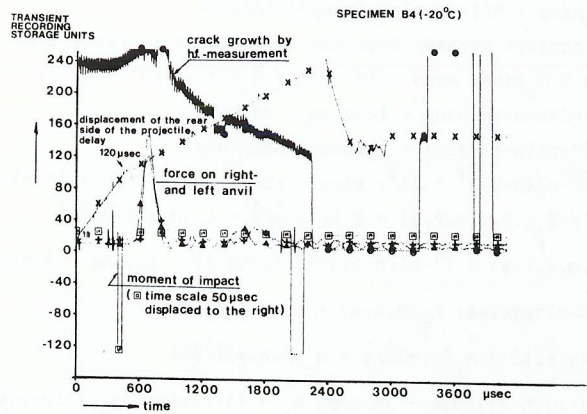


Fig. 8. Synchronic electronic recordings of response from: X photocell array to projectile position; □ impact detecting wire; ▲ straingages on support; ● high frequency electrical resistance change.

1. the rather momentaneous drop in projectile velocity at impact in a quantitative way. The expected time discrepancy of (length of projectile = 600 mm)/(sound velocity = 5 mm/μsec) = 120 μsec between the signal of a wire contacting the specimen at impact and the signal of the rear of the projectile indicating projectile velocity change was clearly revealed; conversely the wire impact signal could serve to precise the location of the velocity change in the projectile path vs. time recording.
2. the high frequency current measurement over the notch, revealing the crack extension. (The sampling frequency of the transient recorder measuring the demodulated primary current of the transformer as elaborated before, has to be such that aliasing with the tuning frequency remained acceptable).
3. the response of the straingages glued on the supports to the load exerted by the specimen on these.

Examples of typical R-evaluations are given in Tables 2a and 2b, using ϕ and a plotted as a function of time according to the high speed photographic recordings and fitted by a polynomial of 2nd degree (Fig. 9a and 9b). This allows to find $W_2(a)$ according to (2); r was taken 0,45. A time polynomial fitting of W_2 offers by differentiation \dot{W}_2 and therewith $R(a, \dot{a}) = \dot{W}_2(a, \dot{a}) / b \dot{a}$. In Fig. 10 $W_2(a)$ is plotted as a function of temperature for the 4 linepipe steels.

DISCUSSION

Surprisingly the R-values in a single gasgun high velocity impact test were gratifyingly reproducible in a certain a -interval. Related and corroborating results with DWT-tests were obtained by Fearnhough, Dickson and Jones (1976). Such a "plateau" in the $R(a)$ -behaviour usually proved far less pronounced in instrumented displacement controlled hydraulically performed tests on notched linepipe specimens with ductile crack extension velocities of ca. 10 mm/sec. For this latter case a multiple test piece method with varying initial ligament in which the average dissipated energy per unit crack area for total separation $W/(h-a_0)$ can be determined, was then consequently required for an R-estimate.

TABLE 2a Specimen A2 (16 mm), test temperature 20°C; $m_1 = 5.403$ kg; $v_{10} = 79.38$ m/sec; $\frac{1}{2}m_1v_{10}^2 = 17.023$ kJ; $v_1 = 42.4$ m/sec; $b_0 = 0.0168$ m; $h_0 = 0.0973$ m; $m_2 = 3.902$ kg; $\frac{1}{2}q = 0.1365$ m; $I_2 = 0.02182$ kgm².

a [mm]	t [μsec]	ϕ [rad]	$\dot{\phi}$ [rad/sec]	P_3 [Ns]	\dot{a} [m/sec]	W_2 [kJ]	$R = \dot{W}_2 / b \dot{a}$ [MN/m]
20	320	0.0836	284	58	120	8.66	1.59
30	405	0.1076	280	72	110	9.28	1.60
40	500	0.1340	276	94	100	9.60	1.58
50	605	0.1627	271	99	90	9.66	1.55
60	730	0.1962	265	106	75	9.80	1.56
70	890	0.2379	257	122	55	10.13	1.61
80	1155	0.3043	244	132	20	10.55	2.05

TABLE 2b Specimen B1 (30 mm), test temperature 20°C; $m_1 = 5.700$ kg; $v_{10} = 81.0$ m/sec; $\frac{1}{2}m_1v_{10}^2 = 18.700$ kJ; $v_1 = 32.5$ m/sec; $b_0 = 0.0304$ m; $h_0 = 0.097$ m; $m_2 = 5.829$ kg; $\frac{1}{2}q = 0.1220$ m; $I_2 = 0.03135$ kgm².

a [mm]	t [μsec]	ϕ [rad]	$\dot{\phi}$ [rad/sec]	P_3 [Ns]	\dot{a} [m/sec]	W_2 [kJ]	$R = \dot{W}_2 / b \dot{a}$ [MN/m]
20	220	0.0521	174	0	95	11.42	1.17
30	310	0.0677	172	10	75	11.65	1.38
40	450	0.0914	167	60	60	12.71	1.54
50	670	0.1275	161	70	45	12.94	1.65
60	930	0.1682	152	80	33	13.21	1.62
70	1260	0.2168	142	95	23	13.57	1.19
80	1800	0.2891	126	105	11	13.89	1.29

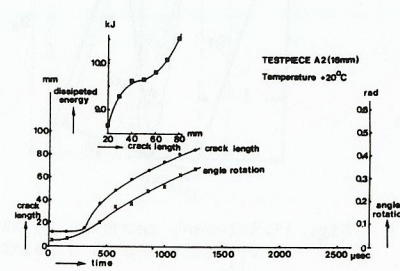


Fig. 9a. Time dependence of cracklength a and rotation ϕ of specimen-half (A2).

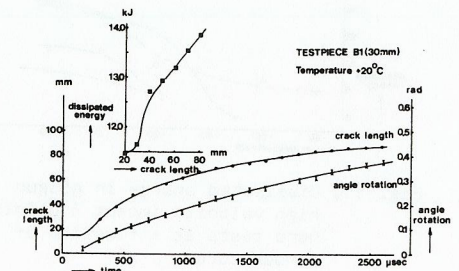


Fig. 9b. Time dependence of cracklength a and rotation ϕ of specimen-half (B1)

It proved that $W/(h-a_0)$ linearly increased with $h-a_0$ and it was demonstrated that its extrapolation to $h-a_0 = 0$ corresponds to the sought for R-value (Van Elst, 1979; Priest and colleagues, 1977, 1978). The increase in the energy dissipation with crack extension evaluated in the gasgun high impact velocity bend test will largely correspond to the decrease of $\zeta^2 \sin^2(\beta+\phi) \dot{\phi}^2$ in (2b), (2c), i.e. to the increase in time of ϕ as recorded by the high speed photographic recordings. The determination of ϕ from the $\phi=\phi(t)$ observations did not allow to detect a significant time dependence of ϕ in presence of the supports; in absence of the supports a decrease in $\dot{\phi}$ is noticeable. At the lower test temperatures and in presence of the supports a slight increase of ϕ occurred though still accompanied by a decrease in \dot{a} ; a disturbing decrease in the described $W_2(a, \dot{a})$ -evaluations then sometimes falsely was found, apparently due to inaccuracy in the $\phi(t)$ -determination and the applied neglects. A more suitable method to determine $\dot{\phi}$ for which a feasible electro magnetic inductive detection, responding to the rotational movement of the specimen halves, readily presents itself, will improve the accuracy in the $\phi(t)$ and $\dot{\phi}(t)$ -recording.

ACKNOWLEDGEMENTS

Centro Sperimentale Metallurgico Rome, delegated part of its work under the European Commission of Steel and Carbon convention 6210/46/4/401 to Metal Research Institute TNO on which is reported above. We thank CSM and ECSC for permission to publish this and mention with appreciation the assistance with the experiments and with the processing of the data by Messrs. W.L. Korbee, M.A. Lont, F.H. Toneman, A. de Bie and F.P.A. van der Hoeven of the Department of Strength of Structural Materials of the Metal Research Institute TNO.

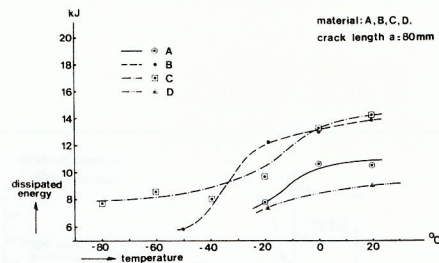


Fig. 10. Dissipated energy in gasgun high velocity impact 3 points bend tests as a function of temperature.

APPENDIX

For the relevant geometry of the impacted 3-points bend specimen the relations between cracklength, deflection and rotation of the assumed rigid specimenhalves read: (cf. Fig. 11)

$$h \cos \phi + (1-r)(h-a) \operatorname{tg} \phi \sin \phi - (S-s) \sin \phi = h-f$$

$$h \sin \phi - (1-r)(h-a) \sin \phi + S \cos \phi = S_0$$

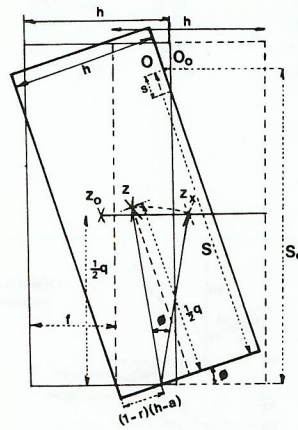


Fig. 11. Relevant geometry in high velocity impact 3 points bend test.

$$s = s(\phi) = \{S_0 \sin \phi - h(1 - \cos \phi) - f \cos \phi\} / \sin \phi \cos \phi$$

Note that if contact between specimen and rollers is kept, i.e. $s = 0$:

$$h = (h-f) \cos \phi + S_0 \sin \phi; \cos \phi = \{h(h-f) + S_0 S\} / \{(h-f)^2 + S_0^2\}; S = \sqrt{S_0^2 - 2fh + f^2}$$

$$x_{z1} = f + (1-r)(h-a) \operatorname{tg} \phi \sin \phi + \frac{1}{2}(h \cos \phi - q \sin \phi)$$

$$y_{z1} = \{\frac{1}{2}h - (1-r)(h-a)\} \sin \phi + \frac{1}{2}q \cos \phi = A \sin(\alpha + \phi)$$

$$A^2 = \{\frac{1}{2}h - (1-r)(h-a)\}^2 + \frac{1}{4}q^2; \sin \alpha = \frac{1}{2}q/A; \cos \alpha = \{\frac{1}{2}h - (1-r)(h-a)\}/A$$

$$\dot{x}_{z1} = \{\xi_{\frac{1}{2}} \dot{f}/\dot{\phi} + \xi_{\frac{1}{2}}(h, q, a, r, \phi) + \xi_{\frac{1}{2}}(r, \phi) \dot{a}/\dot{\phi} + \xi_{\frac{1}{2}}(h, a, \phi) \dot{r}/\dot{\phi}\} \dot{\phi}$$

$$\xi_{\frac{1}{2}} = 1; \xi_{\frac{1}{2}}(h, q, a, r, \phi) = (1-r)(h-a) \sin \phi (2 + \operatorname{tg}^2 \phi) - \frac{1}{2}h \sin \phi - \frac{1}{2}q \cos \phi;$$

$$\xi_{\frac{1}{2}}(r, \phi) = -(1-r) \operatorname{tg} \phi \sin \phi; \xi_{\frac{1}{2}}(h, a, \phi) = -(h-a) \operatorname{tg} \phi \sin \phi$$

$$\dot{y}_{z1} = \{\eta_{\frac{1}{2}}(h, q, a, r, \phi) + \eta_{\frac{1}{2}}(r, \phi) \dot{a}/\dot{\phi} + \eta_{\frac{1}{2}}(h, a, \phi) \dot{r}/\dot{\phi}\} \dot{\phi}$$

$$\eta_{\frac{1}{2}} = \{\frac{1}{2}h - (1-r)(h-a)\} \cos \phi - \frac{1}{2}q \sin \phi; \eta_{\frac{1}{2}} = (1-r) \sin \phi; \eta_{\frac{1}{2}} = (h-a) \sin \phi$$

$$\dot{y}_{z1} = \{\frac{1}{2}h - (1-r)(h-a)\} \cos \phi \dot{\phi} + \{-\frac{1}{2}q \dot{\phi} + (1-r) \dot{a} + (h-a) \dot{r}\} \sin \phi = B \sin(\beta + \phi)$$

$$B^2 = \{\frac{1}{2}h - (1-r)(h-a)\}^2 \dot{\phi}^2 + \{-\frac{1}{2}q \dot{\phi} + (1-r) \dot{a} + (h-a) \dot{r}\}^2 \equiv \zeta^2 \dot{\phi}^2$$

$$\zeta \sin(\beta + \phi) = \eta_{\frac{1}{2}} + \eta_{\frac{1}{2}} \dot{a}/\dot{\phi} + \eta_{\frac{1}{2}} \dot{r}/\dot{\phi}; \zeta \sin \beta = \frac{1}{2}h - (1-r)(h-a);$$

$$\zeta \cos \beta = \frac{1}{2}q + (1-r) \dot{a}/\dot{\phi} + (h-a) \dot{r}/\dot{\phi} \text{ (N.B. if } \dot{a} = \dot{r} = 0, \text{ then } B^* = A^* \dot{\phi} = \zeta^* \dot{\phi}^2)$$

$$\ddot{y}_{z1} \equiv D \cos \phi + E \sin \phi \equiv C \sin(\gamma + \phi); C^2 = D^2 + E^2$$

$$D \equiv [\{\frac{1}{2}h - (1-r)(h-a)\} \dot{\phi}^2 - \frac{1}{2}q \dot{\phi}^2 + 2(h-a) \dot{r} \dot{\phi} + 2(1-r) \dot{a} \dot{\phi}];$$

$$E \equiv [-\frac{1}{2}q \dot{\phi} + (1-r) \dot{a} + (h-a) \dot{r} - \{\frac{1}{2}h - (1-r)(h-a)\} \dot{\phi}^2 - 2 \dot{a} \dot{\phi}].$$

If $\ddot{\phi}$, \ddot{a} , \ddot{r} , \ddot{r} can be neglected in the considered a-interval:

$$C \sin \gamma = D \approx -\frac{1}{2}q \omega^2 + 2(1-r) \dot{a} \omega; C \cos \gamma = E \approx \{\frac{1}{2}h - (1-r)(h-a)\} \omega^2$$

REFERENCES

Cotterell, B. (1977). Plane stress ductile fracture. Proc. of an int. conf. on Fracture Mechanics and Technology, 785-795, Hong Kong, Ed. by G.C. Sih and C.L. Chow at Sythoff and Noordhoff International Publishers.

Dick, J.A., P. Mck. Jamieson and E.F. Walker (1974). The prediction of toughness requirements for the arrest of unstable fracture in pipelines. Proc. 1st Int. Conf. on Crack Propagation in Pipelines, paper 15, British Gas Corporation and The Institution of Gas Engineers, New Castle upon Tyne, England.

Elst, H.C. van (1974). Criteria for steady state crack extension in gas pipelines. Proc. of an int. conf. on Prospects of Fracture Mechanics, 299-318, Delft, The Netherlands. Ed. by G.C. Sih, H.C. van Elst, D. Broek at Noordhoff International Publishing, Leyden.

Elst, H.C. van (1979). Characterization of fracture toughness at crack extension by developed deformation; comparison with energy balance considerations. Proc. of an int. conf. on Fracture Mechanics in Engineering Application, 781-808, Bangalore, India. Ed. by G.C. Sih and S.R. Valluri at Sythoff Noordhoff, Alphen a/d Rijn, The Netherlands.

Engl, B. and F. Fuchs (1978). Investigation of the origins of separations and their effect on mechanical behaviour in linepipe steels. Proc. of the AGA-EPRG Linepipe

- Research Seminar III, pres. nr. 13, Houston, Texas, U.S.A.
- Fearnehough, G.D., D. Dickson and D.G. Jones (1976). Dynamic toughness determination in ductile materials. Proc. of the conf. on Dynamic Fracture Toughness, 315-325, London, England; The Welding Institute and ASM Vol. 1.
- Hahn, G.T., M. Sarrate, M.F. Kanninen and A.R. Rosenfield (1973). A model for unstable shear crack propagation in pipes containing gaspressure. Int. Journ. of Fracture, 9, 209-222.
- Junker, G and G. Vogt (1978). Influence on the results of instrumented BDWT-tests. Proc. of the AGA-EPRG Linepipe Research Seminar III, pres. nr. 10, Houston, Texas, U.S.A.
- Maxey, W.A., K.F. Kiefner, F.J. Eiber and A.R. Duffy (1972). Ductile fracture initiation, propagation and arrest in cylindrical vessels. Proc. of the 5th Nat. Symposium on Fracture Mechanics, University of Illinois, U.S.A., Part II ASTM-STP 514, 70-81.
- Poynton, W.A. (1974). A theoretical analysis of shear fracture propagation in back filled gas pipelines. Proc. 1st Int. Conf. on Crack Propagation in Pipelines, paper 14, British Gas Corporation and the Institution of Gas Engineers, New Castle upon Tyne, England.
- Poynton, W.A. and G.D. Fearnehough (1972). An analysis of shear fracture propagation in gas pipelines. Proc. of an int. conf. on Dynamic Crack Propagation, 183-196, Lehigh University, Bethlehem, Pennsylvania, U.S.A. Ed. by G.C. Sih at Noordhoff International Publishing, Leyden, The Netherlands.
- Priest, A., B. Holmes, H.C. van Elst, H. Wildschut and M.A. Lont (1977, 1978). Fracture Behaviour of Linepipe steel. Final reports to ECSC-conventions 6210.KE/6/601 and 7210.KE/6/601, resp. on EPRG-phase IV program.
- Shannon, R.W.E. and A.A. Wells (1974). A study of ductile crack propagation in gas pressurized pipelines. Proc. 1st Int. Conf. on Crack Propagation in Pipelines, paper 17, British Gas Corporation and the Institution of Gas Engineers, New Castle upon Tyne, England.
- Wilkowski, G.M., W.A. Maxey and R.J. Eiber (1978). Evaluation of fracture resistance measurements for linepipe steels. Proc of the AGA-EPRG Linepipe Research Seminar III, pres. nr. 14, Houston, Texas, U.S.A.